

THERMAL COMFORT AND POLLUTANT TRANSPORT PREDICTION IN THE OBJECT ORIENTED ENVIRONMENT SPARK

E. Wurtz*, M. Musy*, J.M. Nataf**

* Laboratoire d'Etude des Phénomènes de Transfert Appliqués au Bâtiment, Université de La Rochelle, avenue Marillac 17042 La Rochelle Cedex 1, France

** Simulation Research Group, Environmental Energy Technologies Division, Lawrence Berkeley National Laboratory, Berkeley, CA 94720, USA

ABSTRACT:

A coarse-grid zonal model of room air convection is formulated and written with the SPARK object-oriented simulation environment. The model consists of a set of coupled equations determined by heat and mass balance on each of the cells into which the room is divided, convection from the room surfaces and radiant exchange among the room surfaces. The equations are first written in MAPLE, from where they are automatically translated into SPARK objects. The objects are connected to build the simulation. The resulting set of equations is solved iteratively with SPARK to determine the room air flow and temperature distributions. The last but one stage has been automated. So, the only thing the user has to do is to give the partitioning and to choose the models to be implemented. Representing a whole building using zonal models is now possible. Results of simulations in 3D-rooms will be presented.

INTRODUCTION

Room convection models are needed that are intermediate between single-air-node models, which give no information about air flow patterns, and CFD models, which give detailed temperature and flow distributions but are extremely compute intensive. Such intermediate models execute much faster than CFD calculations but give more accurate heat transfers than the single-node approach and provide temperature and flow distributions that are accurate enough to predict thermal comfort.

One such intermediate approach is the so-called "zonal model." In zonal models the inside of a room is divided into a small number of zones or "cells" (on the order of 10 to 100, compared to 1000 or higher for typical CFD calculations), which are usually rectangular parallelepipeds. Mass balance and heat balance equations are applied to the cells and the exchanges are calculated between them. The solution of the resulting set of coupled equations gives the air flow and temperature distribution in the room.

The first zonal models [1-4] were based on fixed air flow directions and on the application of specific flow laws for plumes, jets and boundary layers. Allard and Inard [5] have reviewed these models.

Assuming fixed air flow directions obviously restricts the field of application of these models.

Other models [6,7] made the inter-cell air flow rates a function of the pressure distribution. It has been shown that this approach cannot correctly represent the driving flows [8].

Later, hybrid models were formulated that applied specific laws for driving flows and used a power-law pressure distribution everywhere else [9,10]. However, these models are applicable only to a few simple configurations.

In the present work we present an advanced formulation of a zonal model. To achieve a complete thermal calculation we have connected the zonal air flow calculation with conduction through the room walls and radiant interchange between them. This approach allows virtually any geometrical configuration to be modeled by assembling calculation elements from a model library. This is automatically done using the pre-processor called GENSPARK we have designed. From few information about the building to model, GENSPARK produce all the SPARK files necessary to launch the simulation in SPARK[11] object-oriented environment.

DESCRIPTION OF THE MODEL

Applying the zonal model to a building involves dividing it into rooms and partitioning the rooms into "cells". Equations for mass balance and heat balance are written for each cell. Additional equations describe conduction through the walls, convection between inside wall surfaces and cells, and long-wave and short-wave radiant interchange among the inside wall surfaces. The equations are grouped into small set of equations which are the elements constituting the model library

In the zonal air flow model four different types of cells are considered: basic cells (with low air flow), plume cells, jet cells and boundary-layer cells. Each type of cell has a different set of equations for the internal behavior of the cell and for the transfer with other cells.

Assuming that air is incompressible, the sum of the mass flows across the faces of a cell must be zero. This yields the following mass balance equation for a

basic cell (the geometry of a cell is shown in figure 2):

$$Q_{mWest} - Q_{mEast} + Q_{mSouth} - Q_{mNorth} - Q_{mTop} + Q_{mBottom} = 0 \quad (1)$$

Similarly, the net heat transferred into the cell across its faces must equal the heat stored in the volume of air in the cell. This yields the following heat balance equation for a basic cell:

$$\Phi_{East} - \Phi_{West} + \Phi_{North} - \Phi_{South} + \Phi_{Top} - \Phi_{Bottom} = \Phi_{source} - h w L c_p \rho_i \frac{\partial T_i}{\partial t} \quad (2)$$

Finally, we assume that the relationship between the air pressure, density and temperature in a basic cell is given by the perfect gas law:

$$P_i = r \rho_i T_i \quad (3)$$

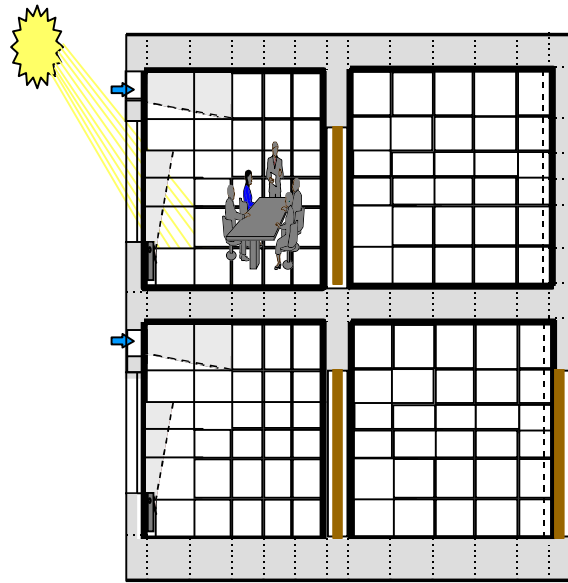


Figure 1 : zonal model applied to a building

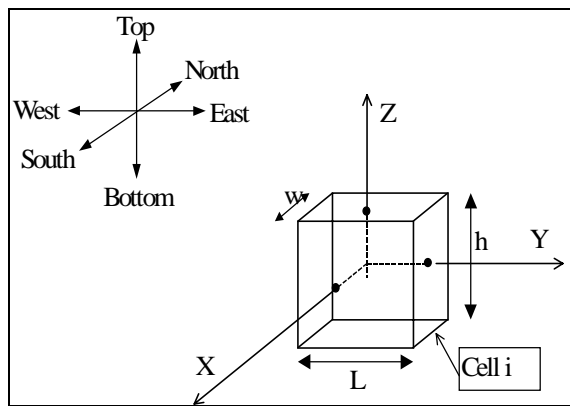


Figure 1: Geometry of a cell in the zonal model.

For vertical faces the mass flow rate is assumed to be proportional to the pressure difference across the face. Therefore, the mass flow rate across the east fact, for example, is given by

$$Q_{mEast} = -C(P_i - P_{East}) \quad (4)$$

For horizontal faces the hydrostatic variation of pressure is taken into account. Therefore, the mass flow rate across the bottom face, for example, is given by

$$Q_{mBottom} = -C \left((P_i - P_{Bottom}) - \frac{1}{2} g (\rho_{Bottom} h_{Bottom} + \rho_i h_i) \right) \quad (5)$$

The overall heat exchange across a face is the sum of the enthalpy flux and conductive flux, giving, for example, for the east face

$$\Phi_{East} = (T_{East} Q_{mEast} + T_i Q_{mEast}) - \frac{\lambda h L}{c_p w} (T_{East} - T_i) \quad (6)$$

The macro calculation objects associated with cells and with interfaces between cells are shown schematically in figures 3 and 4, respectively. For example, figure 4 shows that the interface variables Q , Φ , L and w are shared with the two cells on either side of the interface. Thus, for a horizontal interface, the mass flow variable Q is linked to the variable Q_{bottom} of the cell above the interface and to the variable

Q_{top} of the cell below the interface. Similarly, T_2 is linked to the temperature variable T of the cell above the interface and T_1 to the temperature variable T of the cell below the interface.

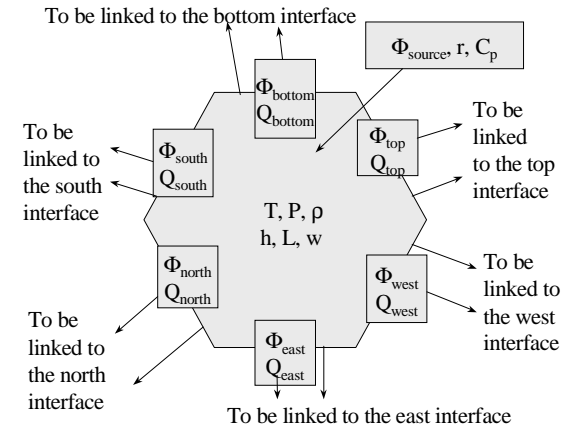


Figure 3 : Schematic representation of a macro-object for a basic cell with six faces.

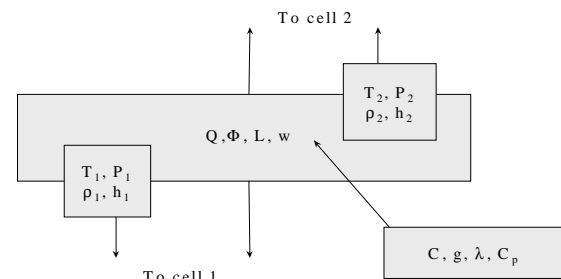


Figure 4 : Schematic representation of a macro-object for a basic interface between cells.

Our approach of particular air is exemplified by the thermal plume case.

A plume is a region of rising warm air such as that produced by a convective heater next to a wall (figure 5). We assume that a plume does not develop laterally as it rises but entrains air through its side faces. The plume model incorporates five calculation objects. The heater is represented by a *heater cell*. A *heater/wall interface* describes the thermal exchange between the back of the heater and the wall. The plume itself is represented by a *plume cell*, a *horizontal plume interface* and a *vertical plume interface* (figure 6).

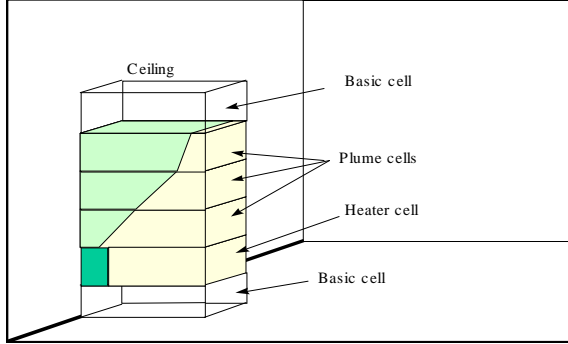


Figure 5: Cells associated with the plume model.

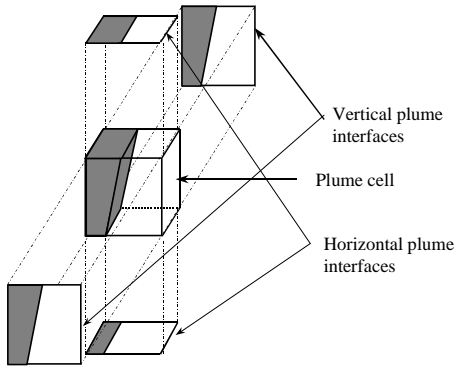


Figure 6: A plume cell and its interfaces. A plume cell contains two subcells and their corresponding subinterfaces. One of these subcells (shaded) contains air from the plume and the other (unshaded) contains surrounding air.

A plume cell contains two subcells, one containing air belonging to the plume itself and one containing air from the surroundings. This type of partitioning is also done for a heater cell. For this reason, the plume and heater objects consist of equations that are reused from the basic cell object (to represent the surrounding air) plus additional equations that are specific to the plume or heater. These objects link to their neighbors in the same way that basic cells link except that there are additional links.

Note that the heater and its associated plume are contained in rectangular parallelepipeds of the same size and shape stacked on top of each other. This simplifies partitioning of a room that has plumes

since it makes it easy to “line up” the plume and heater cells with the other cells in the room.

In the following we describe the thermal characteristics of a plume using the equations of Inard *et al.* [12]. For horizontal interfaces the plume width is

$$Bu = \frac{2E_0}{\sqrt{\pi}} \left(1 + \frac{St(1+\lambda^2)^{1/2}}{3\lambda E_0} \right) (z - z_0) \quad (7)$$

The maximum plume velocity is

$$Um = \left(\frac{6\lambda(1+\lambda^2)^{1/2}}{3\lambda(Cf + \sqrt{2}(E_0 - (1+\lambda^2)^{1/2}St))} \right)^{1/3} \left(\frac{\varphi(z)g\beta}{\rho_0 Cp} \right)^{1/3} \quad (8)$$

where $\varphi(z)$ is the horizontal heat flux into a plume cell.

The plume air flow rate is

$$q = \frac{\sqrt{\pi}}{2} \rho_0 Um Bu \quad (9)$$

The maximum temperature difference between the midpoint of a plume cell and the mean room air temperature is given by

$$\Delta Tm = \left(\frac{\varphi(z)g\beta}{\rho_0 Cp} \right)^{1/3} \left(\frac{3}{2St(1+\lambda^2)^{1/2} + 6\lambda E_0} \right) \left(\frac{1}{g\beta(z - z_0)} \right) \left(\frac{4(1+\lambda^2)}{3\lambda} (3\lambda(Cf + \sqrt{2}E_0) - (2(1+\lambda^2))^{1/2}St) \right)^{1/3} \quad (10)$$

Here $\varphi(z)$ is the average of the heat fluxes crossing the upper and lower interfaces of the subcell that contains the plume (see figure 6). These heat fluxes are determined using the energy balance equation applied to the subcell. The mass balance equation also allows the flow rate of air entrained by the plume to be calculated. This flow rate is assumed to be the same on all faces (front and lateral) of the plume.

The top of the plume (i.e., the point at which the plume has dissipated) is defined to be the height at which $\varphi(z)$ becomes less than a threshold value. Above this height, Bu , Um and ΔTm are set to zero and the cells revert back to basic cells. Therefore, it is not necessary to know a priori how high the plume will reach: the simulation will automatically convert plume cells to basic cells above the dissipation point.

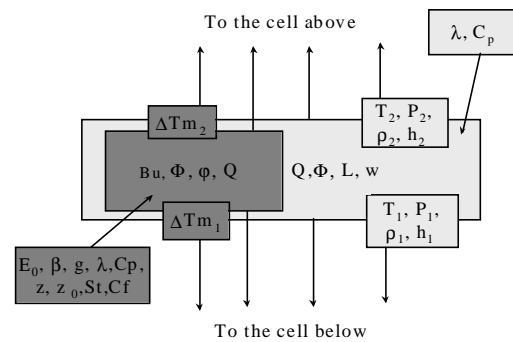


Figure 7: Schematic representation of a horizontal

interface of a plume cell.

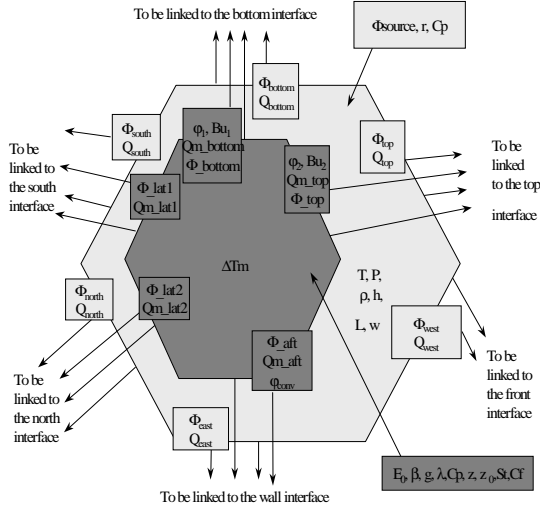


Figure 8: Schematic representation of a plume cell object.

For the heater cell, the temperatures of the front and back surfaces of the heater (figure 8) are given by the following equations [13,14]:

$$T_{front_face} = 0.67 \left(\frac{P_{elec}}{P_{nom}} \Delta T_{s_{max}} \right) + T_a \quad (11)$$

$$T_{back_face} = \frac{P_{elec}}{P_{nom}} (0.67 \Delta T_{s_{max}} - 7) + T_a \quad (12)$$

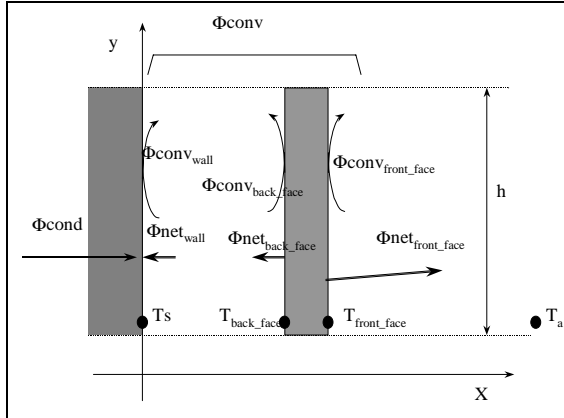


Figure 9 : Heater model.

The sum of the convective and radiative flux from the heater is set equal to the heater input power:

$$P_{elec} = \Phi_{conv_back_face} + \Phi_{conv_front_face} + \Phi_{rad_back_face} + \Phi_{rad_front_face} \quad (13)$$

It is assumed that the convective flux from the heater goes entirely into the plume. The back face of the heater is assumed to radiate only to the wall behind the heater, giving

$$\Phi_{net_wall} = -\Phi_{net_back} = \frac{\epsilon_{heater} \epsilon_{LW_wall} S \sigma (T_s^4 - T_{back_face}^4)}{\epsilon_{heater} + \epsilon_{LW_wall} - \epsilon_{heater} \epsilon_{LW_wall}} \quad (14)$$

The front face of the heater radiates to the other surfaces of the room.

The convective exchange along the wall behind the heater is calculated using the following expression, in which the empirical coefficient, α , depends on the type of heater [4]:

$$\Phi_{conv_wall} = \alpha \frac{S \left(\frac{(T_{back_face} + T_s) - T_a}{2} \right)^{5/4}}{h^{1/4}} \quad (15)$$

The wall model is now briefly described.

Wall conduction, assumed to be one dimensional, is calculated with finite difference equations. The convective flux at the inside wall surface is

$$\varphi_{conv} = h(T_i - T_{s_i}) \quad (16)$$

where the convective heat transfer coefficient, h , depends on the surface-to-air temperature difference according to:

$$h = C(T_i - T_{s_i})^n \quad (17)$$

for which the values of the coefficient, C , and exponent, n , are given in Table 1.

Table 1: Values of the coefficient and exponent in the expression for convective heat transfer coefficient (eq. 17), for h in W/m^2-K and temperature difference in K.

		C	N
Ceiling	natural convection [15]	3.0	0
	mixed convection [4]	3.0	0.7
Roof	heating roof [16]	1.5	1/3
	other cases [15]	3.0	0
walls	natural convection [15]	1.5	1/3
	mixed convection [17]	3	1/3
	plume aft face [4]	0.662	0.77

We use Walton's method [18] to calculate long- and short-wave radiant exchange among the inside room surfaces. In this method each room surface is assumed to radiate to a fictitious surface (figure 10) whose area, emissivity and temperature give about the same heat transfer from the room surface as in the actual multi-surface case. The advantage of the method is that it considerably reduces the number of interchange equations.

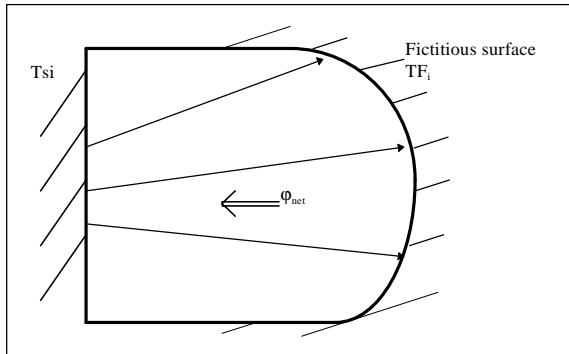


Figure 10: Fictitious-surface method for calculating radiant exchange among room surfaces. A wall with temperature T_{s_i} exchanges radiation with a single fictitious surface with temperature T_{F_i} .

OBJECT-ORIENTED SIMULATION

To solve the zonal model equations we used the Simulation Problem Analysis and Research Kernel (SPARK) [11], a modular simulation environment that automates writing code for systems of non-linear algebraic and differential equations. SPARK allows user to build complex simulations by connecting atomic objects (single equations) or macro-objects (sets of equations). Using graph-theoretic techniques, SPARK reduces the size of the equations system by determining a near-minimum set of iteration variables from which the other unknowns can be calculated. SPARK uses Newton-Raphson iteration to solve this reduced system and, after convergence, solves for the remaining unknowns. SPARK can automatically generate computer code for objects from equations expressed symbolically.

For solution with SPARK we grouped the zonal model equations into cell macro-objects (basic, plume, jet, and boundary layer), interface macro-objects (basic horizontal and vertical, plume, jet, and boundary layer), and a radiant exchange macro-object. These macro-objects were stored in a library for later use.

Cell and interface objects were instantiated as many times as required by the partitioning of the room into individual cells. Then, these objects were linked (the links being the variables shared by the equations corresponding to the objects). Next, the wall interfaces were linked to the radiant exchange macro-object. Finally, input values were specified and SPARK was allowed to determine the unknown variables by iteratively solving the resulting set of several hundred coupled, non-linear equations.

A preprocessor code, called GENSPARK was written that automates the above procedure and embodies the schemata in figures 3, 4, 7 and 8. To create this code the variables of each macro-object were categorized as either local variables shared with neighboring cells neighbors, or as global variables appearing in the cells only or in both the cells and interfaces. Then,

based on the partitioning of the room and on the kind of cells and interfaces involved, the code automatically instantiates the needed macro-objects and links them. All the user has to do is choose the macro-object models, specify how the room is partitioned and enter input parameters.

RESULTS

The first simulation studied here is room [19] equipped with an electrical heater. The inputs to the simulation are the power of the heater and the inside surface temperatures. Figure 11 gives the simulation results. Figure 12 compares measured and simulated air temperature vs. height along the vertical centerline of the room. Simulation agrees with measurement to within 1°C in the three bottom layers and to within 1.3°C in the top layer. However, the agreement in the top layer may be better than this since it is likely that the actual temperature here is higher than the average of the measured temperatures shown at points 6 and 7 in the figure.

Note from this figure that the air temperature difference from floor to ceiling is about 7°C whereas the ceiling surface to floor surface temperature difference is only $23.6 - 21.1 = 2.5^\circ\text{C}$.

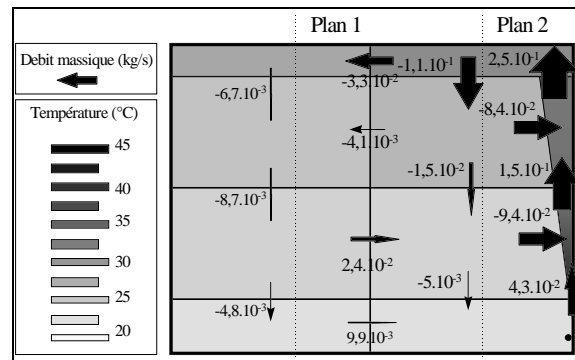


Figure 11: Calculated temperature and air flow values in the East-West vertical plane passing through the heater. On the right side of this plot there is a heater cell at the bottom with two plume cells above it, followed by a basic cell at the ceiling. On the left side of both plots there are four basic cells from floor to ceiling. Shading shows the different temperature levels. Air flow rate is proportional to arrow thickness. Note that this is a section of the room, it is why the mass balance equation seems not to be respected in some cells.

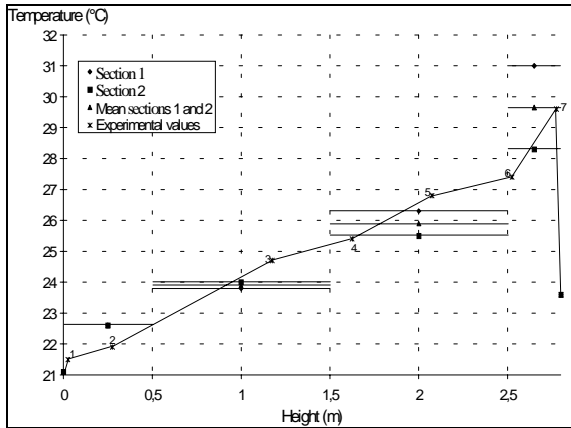


Figure 12 : Comparison of the measured temperature along the vertical centerline of the test room with the results of the simulation. The calculated temperatures are assumed to be uniform in each cell and are therefore shown as horizontal line segments. In this plot the centerline temperatures (solid triangles) have been calculated as the mean of the Section 1 and Section 2 temperatures (see figure 11). The air temperature increases by about 7°C from floor to ceiling, there is significant stratification. For comparison, the temperature difference between the

ceiling surface and floor surface is only $23.6 - 21.1 = 2.5^{\circ}\text{C}$.

The second simulation is a four rooms building. Rooms 1 to 3 are identical. Room 4 is an atrium. Their dimensions are given in figure 13. In South-North direction the thickness of the building is 3 meters. Opened doors separate each small room from the atrium. Rooms 1 to 3 contain heaters. The model constructed consists in 108 cells ($2 \times 3 \times 3$ in rooms 1, 2, 3 and $2 \times 3 \times 9$ in room 4). In each small room, there is an heater cell and a plume cell. The other cells are basic ones. The input data are the wall external surface temperature, the outside air temperature, the power of the heaters and inlet flow rates.

The results in the East-West vertical plane passing through the heaters are given in figure 13.

One can note that in the atrium there is stratification (about 4°C) and that mass exchanges through the doors are significant (mass flow rates are about 6 times greater than the inlet flow rates). The results seem qualitatively correct.

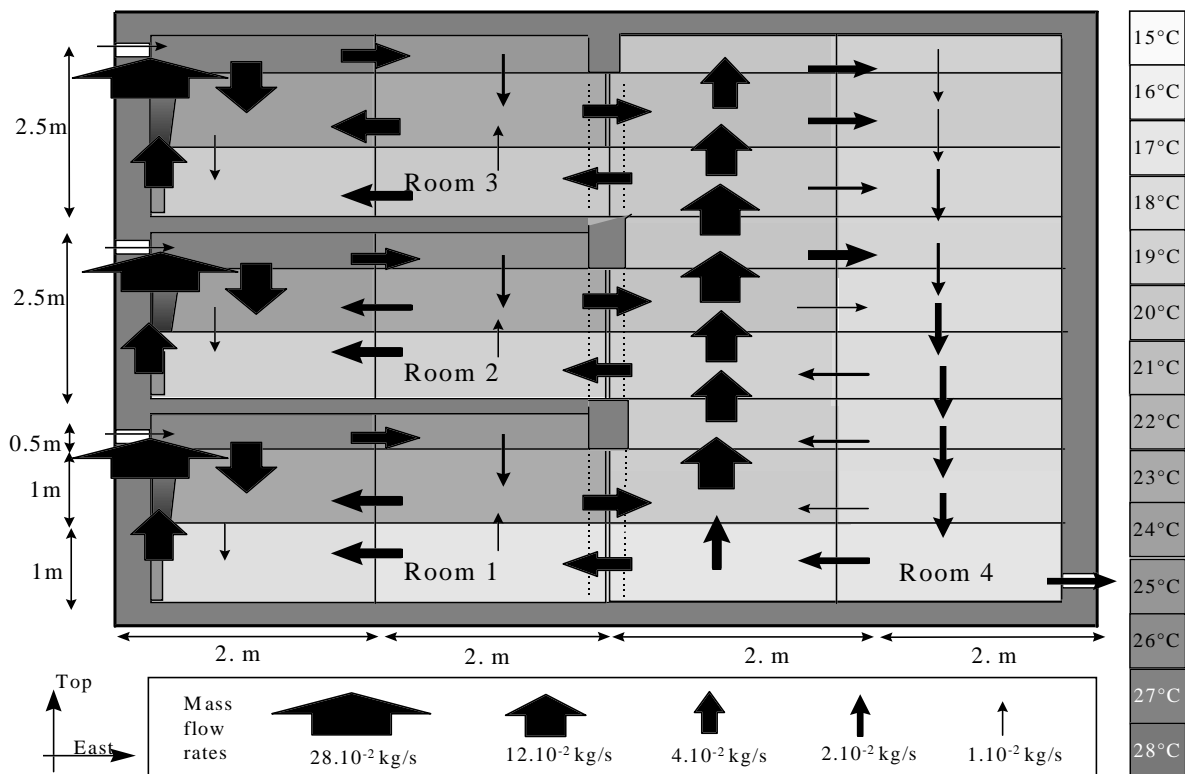


Figure 13 : Calculated temperature and air flow values in the East-West vertical plane passing through the heaters. Shading shows the different temperature levels. Air flow rate is proportional to arrow thickness. Note that this is a section of the room, it is why the mass balance equation seems not to be respected in some cells.

CONCLUSION AND SCOPE

We have shown how a zonal model can be used to calculate room air temperature and air flow distributions. In the cases studied, dividing the room air volume into 24 or 45 cells was sufficiently fine-grained to allow thermal comfort to be determined without excessive calculation time or machine capacity. This will encourage us to use the new PC version of SPARK.

Different levels of automation were used to generate models in the SPARK object-oriented simulation environment:

- Generating equation objects using symbolic processing.
- Automatic generation of SPARK simulation files for a whole building.

This makes it possible to generate a complete simulation of a building given only the building geometry and properties of the heating and cooling systems.

We are currently working on integrating other models for particular flows to allow simulating air conditioning systems. We are also working on taking into account pollutants in the air flow model.

So far, the comparisons we have made with experimental measurement have been encouraging. We are currently making additional comparisons to further validate our zonal model approach.

It is important to note that the simulation approach that we have developed can be applied to all types of thermal and air-flow problems: it is not restricted to simple configurations nor is it required that the flow distribution be known *a priori*.

REFERENCES

[1] J. Lebrun, "Etudes expérimentales des régimes transitoires en chambres climatiques : ajustement des méthodes de calcul". Journées Bilan et Perspectives en Génie Civil. 1978.

[2] L. Laret, "Contribution au développement de modèles mathématiques du comportement thermique transitoire de structures d'habitation". Ph.D. Thesis, University of Liège. 330p. 1980

[3] A.T. Howarth, "The prediction of air temperature variation in naturally ventilated rooms with convective heating". Building Service Engineering Research and Technology. 6(4):169-175, 1985.

[4] C. Inard, "Contribution à l'étude du couplage thermique entre une source de chaleur et un local". Ph.D. Thesis, INSA de Lyon, France. 1988.

[5] F. Allard and C. Inard, "Natural and mixed convection in rooms: prediction of thermal stratification and heat transfer by zonal models". International Symposium of Room Air Convection and Ventilation Effectiveness. University of Tokyo, July 22-24, 1992.

[6] H. Bouia, "Modélisation simplifiée d'écoulements de convection mixte internes: application aux échanges thermo-aérodynamiques dans les locaux". Ph. D. Thesis, University of Poitiers, France, 1993.

[7] E. Wurtz, J.M. Nataf and F. Winkelmann, "Two- and Three-Dimensional Natural and Mixed Convection Simulation Using Modular Zonal

Models". LBL Report, LBNL-39098, Lawrence Berkeley National Laboratory. July 1996.

[8] M. Musy, E. Wurtz, S. Gagneau, "Génération automatisée d'une simulation thermique et aérodynamique dans le bâtiment". Journée « Innovations et perspectives de recherche », Société Française des Thermiciens, November 26, 1997.

[9] A. Grelat, "Approche des phénomènes de circulation et de stratification de l'air dans les locaux chauffés par le programme de simulation thermique multizone BILGA". CEBTP-EDF contract final report, February 1987.

[10] P. Dalicieux, H. Bouia, "Présentation d'une modélisation simplifiée des mouvements d'air à l'intérieur d'une pièce d'habitation". Electricité de France report HE 12 W 3269. 1991.

[11] F. Buhl, E. Erdem, J.M. Nataf, F. Winkelmann and E. Sowell, "Recent improvements in SPARK: Strong component decomposition, multivalued objects and graphical interface". Lawrence Berkeley National Laboratory Report LBL-33906. August 1993.

[12] C. Inard, A. Meslem, P. Depecker, P. Barles, "Structure moyenne et analyse intégrale du panache thermique des convecteurs électriques". Revue Générale de Thermique 36: 495-509, 1997.

[13] P. Barles, "Caractérisation de l'émission des convecteurs électriques - Etude statistique". Centre Technique des Industries Aérodynamiques et Thermiques, CETIAT/ADEME contract report (2.04.005), 1992.

[14] P. Barles, "Contribution du CETIAT aux travaux du sous-groupe convecteurs électriques du GREC". Centre Technique des Industries Aéronautiques et Thermiques, ADEME contract final report (2.04.005), 1993.

[15] F. Allard, "Contribution à l'étude des transferts de chaleur dans les cavités thermiquement entraînées : application aux cellules d'habitation". Thèse de Doctorat ès Sciences, INSA de Lyon, France. 1987.

[16] Kast and Klan, "Auslegung und prüfung von fußbodenheizungen". VDI-Berichte 464: 39-49. 1982.

[17] J. Lebrun, "Exigences physiologiques et modalités physiques de la climatisation par source statique concentrée". Ph.D. Thesis, University of Liège. 1970.

[18] G.N. Walton, "A new algorithm for radiant exchange in room loads calculations", ASHRAE Transactions, vol 86, Part II, pp 190-208; 1980

[19] H. During, "Consommation énergétique et confort thermique des locaux chauffés: approche par les modèles zonaux", Ph.D. thesis, Insa de Lyon, 1994

LIST OF SYMBOLS

Bu : plume width [m]
 C (eq 14): pressure power-law coefficient [$\text{kg}/\text{m}^2\text{-s-Pa}$]
 C (eq 17): coefficient [$\text{W}/\text{m}^2\text{K}^{n+1}$]
 c_p : specific heat of air at constant pressure [$\text{J}/\text{kg-K}$]
 E_0 : entrainment factor
 g : gravitational acceleration [$\text{m}/\text{kg-s}^2$]
 h : cell (or interface) height [m]
 h (eq 16,17): convective heat transfer coefficient [$\text{W}/\text{m}^2\text{K}$]
 L : cell (or interface) length [m]
 w : cell (or interface) width [m]
 n (eq 17): exponent
 P : pressure [Pa]
 P_{elec} : heater electrical power [W]
 P_{nom} : heater nominal power [W]
 Q_m : air flow rate [kg/s]
 r : air molar constant [$\text{m}^2/\text{s}^2\text{K}$]
 S : surface area [m^2]
 St : Stanton number
 T : temperature [K]
 T_a : average room air temperature [C]
 T_s : surface temperature [C]
 U_m : maximum mean plume velocity in a cross section [m/s]

z : altitude [m]
 z_0 : altitude of the beginning of the plume [m]
 β : coefficient of thermal expansion [K^{-1}]
 $\Delta T_{s_{\text{max}}}$: maxim temperature difference between front face of heater and ambient
 ϵ : emissivity
 λ (eq 6): thermal conductivity [W/mK]
 λ (eq 8): ratio between thermal and dynamic plume width
 ρ : air density [kg/m^3]
 σ : Stefan-Boltzmann constant
 ϕ : heat flux [W/m^2]
 ϕ_{conv} : convective heat flux [W/m^2]
 ϕ_{rad} : net radiative heat flux [W/m^2]
 Φ : heat flux [W]
 Φ_{conv} : convective heat loss [W]
 Φ_{rad} : net radiative heat loss [W]
 Φ_{source} : heat source power [W]

Subscripts :

back_face: back face of the heater
front_face: front face of the heater
i: surface i or cell i
wall: wall surface